

Extended analysis of the Ar VII spectrum in the vacuum ultraviolet region

F.O. Borges^{1,a}, F. Bredice², G.H. Cavalcanti¹, M. Gallardo², M. Raineri²,
J.G. Reyna Almandos², and A.G. Trigueiros¹

¹ Instituto de Física, Universidade Federal Fluminense, UFF, Campus da Praia Vermelha-Gragoatá, 24210-340 Niterói, Rio de Janeiro, Brazil

² Centro de Investigaciones Opticas, CIOp, Casilla de Correo 124, B 1902WAB, La Plata, Argentina

Received 28 February 2005 / Received in final form 11 May 2005

Published online 30 August 2005 – © EDP Sciences, Società Italiana di Fisica, Springer-Verlag 2005

Abstract. The analysis of the magnesium-like Ar VII spectrum was extended to include the $3s5s$, $3s6d$, $3p4p$, $3s5p$ and $3p5s$ configurations, in the vacuum ultraviolet region. Sixty-six new transitions have been identified as transitions between the levels of the configurations stated above. Fifteen new levels were determined that belong to these configurations. Hartree-Fock calculations with relativistic corrections were used to predict energy levels, transitions and to support the experimental results.

PACS. 32.30.Jc Visible and ultraviolet spectra – 52.80.Yr Discharges for spectral sources (including inductively coupled plasma)

1 Introduction

Six-times-ionized argon, Ar VII, belongs to the Mg I isoelectronic sequence with a ground state level of $3s^2\ ^1S_0$.

Phillips and Parker published the first experimental results on the Ar VII spectrum [1]. Transitions to the ground state from low-lying levels were presented for Ar VII in atomic energy levels [2]. Livingston et al. [3] and Buchet-Polizac [4] studied Ar VII spectra excited by the beam-foil technique. Lévêque et al. [5] reported the emission spectra of argon produced by discharges in capillary light sources, but classification of the spectral lines was not possible. Lesteven-Vaïsse et al. [6] studied the high-resolution VUV spectroscopy of Ar with recoil ion spectroscopy and reported results for the low configurations of Ar VII. Fawcett et al. [7] used a theta-pinch plasma to analyze the spectrum of Ar IX and extended the spectral classification in Ar V to Ar VII and Ar X. Boduch et al. [8] obtained results for the Ar VII spectrum using an ECR ion source. Bliman et al. [9–11] used ion-collision spectroscopy to study highly excited levels in Ar VII spectrum. Trigueiros et al. [12, 13], using a theta-pinch as a light source, studied the Ar VII spectrum and presented an analysis of transitions and energy levels in the $n = 3$ complex. The Ar VII spectrum has been the focus of some theoretical calculations [14–16]. In this work we report additional experimental results for the Ar VII spectrum in the VUV region. In these results we include 15 new energy levels and 66

new transitions. This study is a continuation of our investigations of different argon ion spectra using a capillary pulsed discharge as the light source. The interest in spectroscopy data for rare gases is due to applications in collision physics, laser physics, photoelectron spectroscopy, and fusion diagnostics.

2 Experiment

The light source used in our experiment is a Pyrex tube, 120 cm long and with an inner diameter of 0.5 cm. The tube has two inner electrodes of indium and the distance between them is 90 cm. The excitation of the gas is produced by discharging a bank of low-inductance capacitors of 218 μF . Ilford Q-2 plates were used to record the spectra and the known lines of C, N, O, and Ar provided internal wavelength standards. Light emitted axially was analysed using a 3-m normal incidence HILGER & WATTS vacuum spectrograph with a BAUSCH & LOMB concave diffraction grating of 1200 lines/mm, blazed for 1200 Å. The plate factor in the first order is 2.77 Å/mm. To measure the spectrograms a photoelectric semi-automatic Grant comparator was used. This comparator works semi-automatically and permits determination of asymmetric lines through an oscilloscopy display. We studied the behaviour of the spectral line intensities as a function of gas pressure, number of discharges and discharge voltage to distinguish between different states of ionisation. A well-developed Ar VII spectrum was obtained with the following parameters: ± 20 mTorr, 210 discharges, and 16 kV.

^a e-mail: borges@if.uff.br

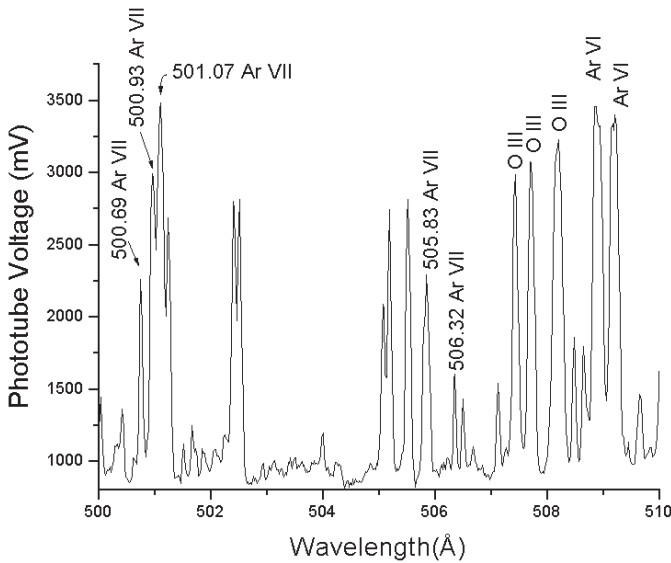


Fig. 1. Spectrum of Ar in 500–510 Å emitted by our discharge source under the following condition: ± 20 mTorr, 210 discharges, and 16 kV. The Ar VII lines are denoted by their ionisation stages and wavelength values. The new lines observed in this range were: 500.93, 505.83 and 506.32.

Figure 1 shows part of the argon spectrum from 500 to 510 Å. The accuracy of the wavelength values for unperturbed lines is estimated to be ± 0.03 Å, and this is based on the agreement for the calibration lines.

3 Analysis

Table 1 presents 66 new laboratory wavelengths for transitions in Ar VII. The experimental intensities of the lines in Table 1 are based on visual estimates of the photographic blackening of the plates and of the amplitude of the electronic signal provided by the comparator. Their values are normalized and vary from 20 to 100.

The line identifications were guided by theoretical predictions that were obtained with the Cowan [17] computer codes. We obtained the predictions by diagonalizing the energy matrices with the appropriate Hartree-Fock Relativistic (HFR) values for the energy parameters. The configuration average energies are shifted by $+9372$ cm^{-1} (the value -9372 cm^{-1} correspond to the $3s^2$ 1S_0 ground-state energy in the calculation). This was done to bring the $3s^2$ 1S_0 ground-state energy to zero, which, of course, must be done. This procedure has practical importance because the calculated energy-level values will be closer to the experimental determined ones.

The level structure was theoretically interpreted by using ab initio estimates of energies and transition probabilities. Also, semi-empirical techniques were used to improve the results of the theoretical calculations. The HFR programs were used to predict wavelengths, energy levels, and relative intensities. By scaling the electrostatic radial integrals by 85% and using the spin-orbit integrals,

without scaling, we found minimum variation between calculated and experimental values. The configurations reported here, do not have isoelectronic experimental data in the Mg I sequence for comparisons.

For studying the even-parity configurations, the $3s5s$, $3s6d$, and $3p4p$ configurations are the subject of our analysis. To take into account most of the configuration interactions we include the following configurations in the calculation of the even-parity levels $3s^2$, $3p^2$, $3s4s$, $3s3d$, $3s4d$, $3s5d$, $3p4f$, $3d^2$, $3d4s$, $3d4d$, and $4f^2$. For the odd-parity case we study the $3s5p$ and $3p5s$ configurations. We include the following configurations in the ab initio calculation of the odd-parity states: $3s3p$, $3s4p$, $3s6p$, $3s7p$, $3p3d$, $3p4d$, $3p5d$, $3p4s$, $3s4f$, $3s5f$, $3d4p$, $3d5p$, $3d4f$, and $3d5f$.

The experimental energy level values derived from the observed lines and the semi-empirical calculated energy level values for the $3s5s$, $3p4p$, $3s5p$, $3p5s$ configurations and one level of $3s6d$ configuration, that was unknown, are given in Table 2. The experimental values were determined in a interactive procedure where the wavenumbers of the observed lines are weighted in accordance to their estimated uncertainties [18]. In our case the uncertainties of the experimental energy level values are less than 7 cm^{-1} . The calculated level values were obtained by the least-squares fit [19,20]. The procedure of the least-squares fit is described in Cowan's book [17]. In this process, the Slater parameters were fitted to the experimental energy level, which should improve the wave function composition as well as the energy separations between the levels. Our calculations included all energy levels experimentally known. All level designations in Table 2 are in LS notation, and in the same table we present the percentage composition of the levels.

In the even-parity configurations the energy level $715\,739 \pm 4$ cm^{-1} ($3s5s$ 3S_1) was determined by Fawcett et al. [7] with three transitions. We confirm this value with six new transitions. The level $3s6d$ 1D_2 has not been established previously. We determined this value to be $842\,309 \pm 4$ cm^{-1} with two strong transitions. The other strong transitions ($3s6d$ $^1D_2 \rightarrow 3p3d$ 1P_1 , 1D_2 , $3s4p$ 1P_1 , and $3s3p$ 1P_1) are below the spectral range observed by us. The $3p4p$ configuration, completely unknown, was studied by us. We determined six of the ten predicted levels for this configuration.

In the odd-parity configurations, the previously known energy level value of $741\,840 \pm 3$ cm^{-1} ($3s5p$ 1P_1) reported by Fawcett et al. [7] was confirmed. Fawcett established this level based on just one transition, we confirmed his result by examining four new transitions with the $3s4s$ 1S_0 , $3s4d$ 3D_2 , 1D_2 , and $3s6d$ 1D_2 energy levels. The others unknown levels $3s5p$ 3P_0 , 3P_1 , and 3P_2 were determined in this work. As we see in Table 2 the discrepancies for the $3s5p$ 3P energy levels are much larger than for the other levels that are presented. The $3s5p$ – $3s4d$ interaction is seen to give a configuration mixing between $3s5p$ $^1,^3P$ and $3p4d$ $^1,^3P$. The discrepancies for the $3s5p$ 3P energy levels occur because the experimental values for the $3p4d$ energy levels are unknown, therefore its configuration parameters are fixed in the adjustment. We also determined all of

Table 1. Identified lines of Ar VII.

Intensity ^a	Wavelengths(Å)		Levels (cm ⁻¹) ^b			Transition				
	Obs	Calc	Lower	Upper						
60bl	415.77	415.76	475218	-	715739	3p3d	³ D ₁ ⁰	-	3s5s	³ S ₁
80	417.36	417.35	472284	-	711889	3p3d	³ P ₂ ⁰	-	3p4p	³ P ₂
60	422.53	422.53	475218	-	711889	3p3d	³ D ₁ ⁰	-	3p4p	³ P ₂
100	423.50	423.50	475763	-	711889	3p3d	³ D ₃ ⁰	-	3p4p	³ P ₂
40	426.70	426.71	634695	-	869046	3s4d	³ D ₃	-	3p5s	³ P ₂ ⁰
60	435.65	435.69	472284	-	701806	3p3d	³ P ₂ ⁰	-	3p4p	³ D ₁
60	436.85	436.81	472875	-	701806	3p3d	³ P ₁ ⁰	-	3p4p	³ D ₁
40	438.63	438.60	473810	-	701806	3p3d	³ P ₀ ⁰	-	3p4p	³ D ₁
60	440.61	440.61	475587	-	702547	3p3d	³ D ₂ ⁰	-	3p4p	³ D ₂
40	443.08	443.10	514073	-	739758	3s4s	³ S ₁	-	3s5p	³ P ₂ ⁰
80	469.63	469.62	528904	-	741840	3s4s	¹ S ₀	-	3s5p	¹ P ₁ ⁰
20	474.42	474.43	528904	-	739685	3s4s	¹ S ₀	-	3s5p	³ P ₁ ⁰
80bl	475.73	475.73	510268	-	720470	3p3d	¹ F ₃ ⁰	-	3p4p	¹ D ₂
40	496.00	495.98	510268	-	711889	3p3d	¹ F ₃ ⁰	-	3p4p	³ P ₂
60	500.93	500.91	669409	-	869046	3d ²	³ P ₂	-	3p5s	³ P ₂ ⁰
80	505.83	505.85	517104	-	714790	3p3d	¹ P ₁ ⁰	-	3s5s	¹ S ₀
40	506.32	506.36	669365	-	866853	3d ²	³ P ₁	-	3p5s	³ P ₀ ⁰
20	513.36	513.39	517104	-	711889	3p3d	¹ P ₁ ⁰	-	3p4p	³ P ₂
20	520.11	520.08	510268	-	702547	3p3d	¹ F ₃ ⁰	-	3p4p	³ D ₂
80	551.75	551.76	517104	-	698342	3p3d	¹ P ₁ ⁰	-	3p4p	¹ P ₁
60	557.46	557.46	698342	-	877728	3p4p	¹ P ₁	-	3s7p	¹ P ₁ ⁰
80	572.05	572.05	667499	-	842309	3s4f	¹ F ₃ ⁰	-	3s6d	¹ D ₂
80	579.75	579.73	698342	-	870837	3p4p	¹ P ₁	-	3p5s	¹ P ₁ ⁰
80	604.57	604.54	701806	-	867221	3p4p	³ D ₁	-	3p5s	³ P ₁ ⁰
80	607.24	607.26	702547	-	867221	3p4p	³ D ₂	-	3p5s	³ P ₁ ⁰
60	613.69	613.73	714790	-	877728	3s5s	¹ S ₀	-	3s7p	¹ P ₁ ⁰
80bl	614.80	614.82	708188	-	870837	3p4p	³ S ₁	-	3p5s	¹ P ₁ ⁰
100	621.65	621.67	708188	-	869046	3p4p	³ S ₁	-	3p5s	³ P ₂ ⁰
80	626.61	626.59	707628	-	867221	3d ²	¹ S ₀	-	3p5s	³ P ₁ ⁰
80bl	630.28	630.26	708188	-	866853	3p4p	³ S ₁	-	3p5s	³ P ₀ ⁰
60	635.94	635.90	720470	-	877728	3p4p	¹ D ₂	-	3s7p	¹ P ₁ ⁰
100	636.31	636.31	711889	-	869046	3p4p	³ P ₂	-	3p5s	³ P ₂ ⁰
80bl	640.83	640.83	714790	-	870837	3s5s	¹ S ₀	-	3p5s	¹ P ₁ ⁰
80bl	640.83	640.80	564416	-	720470	3s4p	³ P ₁ ⁰	-	3p4p	¹ D ₂
60	642.08	642.08	564726	-	720470	3s4p	³ P ₂ ⁰	-	3p4p	¹ D ₂
80	652.29	652.29	715739	-	869046	3s5s	³ S ₁	-	3p5s	³ P ₂ ⁰
60	656.04	656.03	714790	-	867221	3s5s	¹ S ₀	-	3p5s	³ P ₁ ⁰
80bl	660.12	660.14	715739	-	867221	3s5s	³ S ₁	-	3p5s	³ P ₁ ⁰
40	660.82	660.84	564416	-	715739	3s4p	³ P ₁ ⁰	-	3s5s	³ S ₁
60	661.76	661.75	715739	-	866853	3s5s	³ S ₁	-	3p5s	³ P ₀ ⁰
80	662.19	662.19	564726	-	715739	3s4p	³ P ₂ ⁰	-	3s5s	³ S ₁
80	665.04	665.04	720470	-	870837	3p4p	¹ D ₂	-	3p5s	¹ P ₁ ⁰
100	679.53	679.52	564726	-	711889	3s4p	³ P ₂ ⁰	-	3p4p	³ P ₂
80bl	692.94	692.96	563879	-	708188	3s4p	³ P ₀ ⁰	-	3p4p	³ S ₁
80	696.81	696.84	571285	-	714790	3s4p	¹ P ₁ ⁰	-	3s5s	¹ S ₀
100	697.04	697.05	564726	-	708188	3s4p	³ P ₂ ⁰	-	3p4p	³ S ₁
100	723.94	723.95	564416	-	702547	3s4p	³ P ₀ ⁰	-	3p4p	³ D ₂
80	725.03	725.02	563879	-	701806	3s4p	³ P ₀ ⁰	-	3p4p	³ D ₁
80	727.85	727.86	564416	-	701806	3s4p	³ P ₁ ⁰	-	3p4p	³ D ₁
60	766.16	766.16	571285	-	701806	3s4p	¹ P ₁ ⁰	-	3p4p	³ D ₁
60	768.79	768.78	739458	-	869535	3s5p	³ P ₀ ⁰	-	3s7s	³ S ₁
80	770.54	770.55	739758	-	869535	3s5p	³ P ₂ ⁰	-	3s7s	³ S ₁
40	774.30	774.31	698342	-	827490	3p4p	¹ P ₁	-	3s6p	¹ P ₁ ⁰
80	787.08	787.05	571285	-	698342	3s4p	¹ P ₁ ⁰	-	3p4p	¹ P ₁
20	800.40	800.36	702547	-	827490	3p4p	³ D ₂	-	3s6p	¹ P ₁ ⁰
40	887.28	887.31	714790	-	827490	3s5s	¹ S ₀	-	3s6p	¹ P ₁ ⁰

Table 1. *Continued.*

Intensity ^a	Wavelengths (Å)		Levels (cm ⁻¹) ^b			Transition
	Obs	Calc	Lower	Upper		
40	932.78	932.78	634634	- 741840	3s4d	³ D ₂ - 3s5p ¹ P ₁ ⁰
80	938.60	938.61	635299	- 741840	3s4d	¹ D ₂ - 3s5p ¹ P ₁ ⁰
60	950.94	950.95	634600	- 739758	3s4d	³ D ₁ - 3s5p ³ P ₂ ⁰
80	951.27	951.26	634634	- 739758	3s4d	³ D ₂ - 3s5p ³ P ₂ ⁰
80	951.62	951.61	634600	- 739685	3s4d	³ D ₁ - 3s5p ³ P ₁ ⁰
100	951.82	951.81	634695	- 739758	3s4d	³ D ₃ - 3s5p ³ P ₂ ⁰
80	951.91	951.92	634634	- 739685	3s4d	³ D ₂ - 3s5p ³ P ₁ ⁰
80	953.68	953.67	634600	- 739458	3s4d	³ D ₁ - 3s5p ³ P ₀ ⁰
80	956.64	956.64	739758	- 844290	3s5p	³ P ₂ ⁰ - 3s6d ³ D ₃
80	995.34	995.33	741840	- 842309	3s5p	¹ P ₁ ⁰ - 3s6d ¹ D ₂

^a “bl” indicates a blended, unresolved line.

^b The energy level values were adjusted by an interactive optimization procedure with observed wavelengths using the program ELCALC [18].

Table 2. Experimental energy level values for the Ar VII.

Configuration	Level	Energy level observed (cm ⁻¹)	Energy level calculated ^a (cm ⁻¹)	Percentage composition in LS coupling ^b
3p4p	¹ P ₁	698 342 ± 4	698 336	91% + 8% 3p4p ³ D
3p4p	³ D ₁	701 806 ± 4	701 814	88% + 8% 3p4p ¹ P
3p4p	³ D ₂	702 547 ± 5	702 537	96%
3p4p	³ D ₃	-	704 134	96%
3p4p	³ S ₁	708 188 ± 4	708 187	60% + 35% 3s5s ³ S
3p4p	³ P ₀	-	710 414	93% + 6% 3d ² ³ P
3p4p	³ P ₁	-	710 938	95%
3p4p	³ P ₂	711 889 ± 5	711 884	98%
3p4p	¹ D ₂	720 470 ± 5	720 467	90%
3p4p	¹ S ₀	-	744 098	73% + 6% 3d ² ¹ S + 10% 3s5s ¹ S
3s5s	¹ S ₀	714 790 ± 4	714 784	82% + 17% 3p4p ³ S
3s5s	³ S ₁	715 739 ± 4 ^c	715 741	82% + 13% 3d ² ¹ S
3s5p	³ P ₀	739 458 ± 4	739 523	98%
3s5p	³ P ₁	739 685 ± 3	739 602	97%
3s5p	³ P ₂	739 758 ± 3	739 785	98%
3s5p	¹ P ₁	741 840 ± 3 ^c	741 838	94% + 4% 3p4d ¹ P
3s6d	¹ D ₂	842 309 ± 4	842 307	84% + 16% 3d4s ¹ D
3p5s	³ P ₀	866 853 ± 6	866 832	97%
3p5s	³ P ₁	867 221 ± 5	867 242	88% + 9% 3p5s ¹ P
3p5s	³ P ₂	869 046 ± 5	869 051	97%
3p5s	¹ P ₁	870 837 ± 5	870 825	85% + 9% 3p4s ³ P

^a Energy level values from the least-squares fitting calculation.

^b Percentages lower than 4% are omitted.

^c These levels were determined by Fawcett et al. [7] and confirmed by this work.

the energy levels for the 3p5s configuration, that were not known previously. The energy level values 3p5s ³P₀, ³P₁, ³P₂, and ¹P₁ are shown in Table 2. The 3s4p and 3p5s configurations were the key for the determination of the 3p4p configuration, due to the high transition probabilities presented between them. In Tables 3 and 4 we compare the fitted and ab initio HFR values for the Slater parameters. The parameters in Tables 3 and 4 have the following

meanings: E_{av} (configuration-average energy); F^2 , G^0 , G^1 and G^2 are frequently referred to as Slater Integrals [21]. “The radial integrals E_{av} , F^k , G^k , ζ , and R^k are considered simply as adjustable parameters, whose values are to be determined empirically so as to give the best possible fit between the calculated eigenvalues and the observed energy levels”, Cowan [17]. The final discrepancy between

Table 3. Atomic energy parameters of least-squares fit for even configurations of Ar VII.

Configuration	Parameter	HFR, cm ⁻¹	Adjusted, cm ⁻¹	Adjust/HFR
3s5s	E_{av}	708 590	714 019	1.01
	$G^0(3s, 5s)$	2 574	2 088	0.81
3s6d	E_{av}	836 004	844 815	1.01
	$G^2(3s, 6d)$	1 627	1 351	0.83
	ζ_{6d}	93 ^a	-	-
3p4p	E_{av}	701 458	709 034	1.01
	$F^2(3p, 4p)$	30 051	27 798	0.93
	$G^0(3p, 4p)$	8 589	8 525	0.99
	$G^2(3p, 4p)$	10 114	10 407	1.03
	ζ_{3p}	1 628 ^a	-	-
	ζ_{4p}	518 ^a	-	-

^a These parameters were kept fixed in the least-squares fitting calculation.

Table 4. Atomic energy parameters of least-squares fit for odd configurations of Ar VII.

Configuration	Parameter	HFR, cm ⁻¹	Adjusted, cm ⁻¹	Adjust/HFR
3s5p	E_{av}	732 546	741 783	1.01
	$G^1(3s, 5p)$	3 654	4 518	1.24
	ζ_{5p}	244	191	0.78
3p5s	E_{av}	851 231	869 926	1.02
	$G^1(3p, 5s)$	3 559	3 641	1.02
	ζ_{3p}	1 637	1 532	0.94

the observed and semi-empirical calculated energies did not exceed 0.02%.

This research was financially supported by the Fundação de Amparo à Pesquisa do Estado do Rio de Janeiro (FAPERJ), Brazil, by the Conselho Nacional de Desenvolvimento Científico e Tecnológico (CNPq), Brazil, and by Consejo Nacional de Investigaciones Científicas y Técnicas (CONICET), Argentina. F.O. Borges thanks Coordenação de Aperfeiçoamento de Pessoal de Nível Superior (CAPES), Brazil, for a fellowship. The Comisión de Investigaciones Científicas de la Provincia de Buenos Aires (CICPBA), Argentina, where F. Bredice, J.G. Reyna Almandos, and M. Raineri are researchers, is also gratefully acknowledged.

References

1. L.W. Phillips, W.L. Parker, Phys. Rev. **60**, 301 (1941)
2. C.E. Moore, *Atomic Energy Levels*, Natl. Bur. Stand., Ref. Data Ser., Circ. No. 467 (U.S. GOP, Washington, D.C., 1971), Vol. I
3. A.E. Livingston, E.H. Pinnington, D.J.G. Irwin, J.A. Kernahan, R.L. Brooks, J. Opt. Soc. Am. **71**, 442 (1981)
4. M.C. Buchet-Poulizac, J.P. Buchet, P. Ceyzeriat, Nucl. Instr. Meth. **202**, 13 (1982)
5. G. Lévêque, S. Girard, J. Robin, J. Phys. France **45**, 665 (1984)
6. I. Lesteven-Vaïsse, F. Folkmann, A. Ben Sitel, M. Chantepie, D. Lecler, Phys. Scripta **38**, 45 (1988)
7. B.C. Fawcett, A. Ridgeley, G.E. Bromage, Phys. Scripta **18**, 315 (1978)
8. P. Boduch, M. Chantepie, D. Hennecart, X. Husson, H. Kucal, D. Lecler, N. Stolterfoht, M. Druetta, B. Fawcett, M. Wilson, Phys. Scripta **45**, 203 (1992)
9. S. Bliman, J.P. Desclaux, D. Hitz, P. Indelicato, P. Marseille, Nucl. Inst. Meth. Phys. Res. B **31**, 330 (1988)
10. S. Bliman, P. Indelicato, D. Hitz, P. Marseille, J.P. Desclaux, J. Phys. B: At. Mol. Opt. Phys. **22**, 2741 (1989)
11. S. Bliman, M. Cornille, B.A. Huber, H. Lebius, A. Langereis, J. Nordgren, R. Bruch, Phys. Rev. A **60**, 2799 (1999)
12. A.G. Trigueiros, A.J. Mania, M. Gallardo, J.G. Reyna Almandos, J. Opt. Soc. Am. B **14**, 2463 (1997)
13. A.G. Trigueiros, F. Callegari, N. Mansur, G.H. Cavalcanti, A.J. Mania, M. Gallardo, J.G. Reyna Almandos, J. Opt. Soc. Am. B **18**, 1718 (2001)
14. L.J. Curtis, P.S. Ramanujam, J. Opt. Soc. Am. **73**, 979 (1983)
15. B.C. Fawcett, At. Data Nucl. Data Tables **28**, 579 (1983)
16. L. Féret, J. Pascale, J. Phys. B: At. Mol. Opt. Phys. **32**, 4175 (1999)
17. R.D. Cowan, *The Theory of Atomic Structure and Spectra* (Univ. California Press, Berkeley, CA, 1981)
18. L.J. Radziemski Jr, V. Kaufman, J. Opt. Soc. Am. **59**, 424 (1969)
19. F.O. Borges, G.H. Cavalcanti, A.G. Trigueiros, J. Quant. Spec. Rad. Trans. **78**, 119 (2003)
20. F.O. Borges, G.H. Cavalcanti, A.G. Trigueiros, C. Jupén, J. Quant. Spec. Rad. Trans. **83**, 751 (2004)
21. J.C. Slater, Phys. Rev. **34**, 1293 (1929)